The Importance of Stratum Corneum Lipid Organization for Proper Barrier Function

3

Annett Schroeter, Adina Eichner, Josefin Mueller, and Reinhard H.H. Neubert

Contents

3.1 Introduction

Obstacles such as the complexity and chemical variability of the lipids present in the stratum corneum (SC), disturbing other material like proteins, ethical issues related to the use of excised human provided by biological material like excised skin, hinder elucidating the molecular morphology of the SC lipid matrix. These difficulties led to an increasing use of synthetic SC lipids in SC research. To allow for a systematic evaluation of the relevance of single ceramide (CER) species, multilamellar model membranes containing simplistic mixtures of synthetic SC lipids represent a suitable approach as shown in numerous previous works (Kessner et al. 2008a, b; Kiselev 2007: Kiselev et al. 2005; Wegener et al. 1997; Zbytovska et al. 2009). Such a systematic determination of the impact of particular CER subclasses is important for a detailed understanding of mechanisms in skin diseases.

A. Schroeter (✉) • A. Eichner
J. Mueller • R.H.H. Neubert
Institute of Pharmacy, Martin Luther University
Halle-Wittenberg, Halle (Saale), Germany
e-mail: annett.schroeter@pharmazie.uni-halle.de;
adina.eichner@pharmazie.uni-halle.de;
josefin.mueller@pharmazie.uni-halle.de;
reinhard.neubert@pharmazie.uni-halle.de

This knowledge supports the development of new therapeutic approaches. In addition, enhanced understanding of the function of different SC lipids in the process of barrier formation helps to develop new carrier systems being able to overcome the penetration barrier more efficiently.

3.1.1 Ceramides of the Stratum Corneum Lipid Matrix

It is generally known that the main constituents, the ceramides (CER), play a key role in the structuring and hence the maintenance of the barrier function of the skin (Coderch et al. 2003; Holleran et al. 1991). They are a group of structurally heterogeneous sphingolipids and consist of a long-chain fatty acid bound to the amino group of a long-chain di- or trihydroxy sphingoid base (sphingosine, phytosphingosine, and 6-hydroxysphingosine). The bound fatty acid of the CER consists predominantly of a very long almost entirely saturated alkyl chain (Wertz et al. 1987) and can be hydroxylated at the α-position to the carbonyl oxygen, at the end of the hydrocarbon chain (ω-position), or it contains no further hydroxyl group (Coderch et al. 2003). The first nomenclature used to label the different CER was based on their mobility in the thin-layer chromatography (Wertz and Downing 1983). As the number of the identified CER increased, this method of labeling was insufficient. Consequently, the nomenclature of the CER is based on their chemical structure and was developed by Motta and coworkers (Motta et al. 1993). In this system the ceramides are labeled with letters, whereby the last letter assigns the type of sphingoid base (*S*… sphingosine, *P*… phytosphingosine, *H*… 6-hydroxysphingosine). The long-chain fatty acid bound to the amino group can be differentiated due to their hydroxylation. This was taken up in the nomenclature as amid-bound fatty acids without a hydroxyl group were labeled with the letter N (=non-hydroxy), while ceramides with an omega- and alpha-hydroxylated fatty acid receive either the letter O or A, respectively. Furthermore, within the group of ceramides, the exceptionally long-chain ω-acyl ceramides exist, which are esterified with a long unsaturated fatty

acid. In line with the way of labeling, these ceramides received the letter *E* (=esterified). Up to now, 12 major CER classes have been identified within the SC lipid matrix (Holleran et al. 2006; Masukawa et al. 2008) (see Fig. 3.1), but detailed information about their specific role for the barrier formation and function of the SC needs to be elucidated. Especially the long-chain CER[EOS], [EOP] and [EOH] are discussed to be of particular relevance because of their unique structure. As mentioned above these CER have in addition to the amidation either a phytosphingosine (P), sphingosine (S), or hydroxysphingosine (H) base, while the ω-hydroxylated fatty acid is esterified with a linoleic acid (EO) in ω-position (Coderch et al. 2003). Due to the esterified fatty acid, those CER have a chain length of 30–32 carbon atoms (Raith et al. 2004). However, in recent years also the short-chain CER such as CER[AP] and CER[NP] have been in the focus of various investigations, and it became evident that these CER seem to play a more important role in the structural organization of the uppermost skin barrier than previously assumed. But, it is most likely the broad distribution of alkyl chain lengths and the heterogeneity in the head groups which guarantee the integrity and functionality of the lipid lamellae of the SC (Norlen 2001).

3.2 Stratum Corneum Lipid Nanostructure Investigated With Neutron Diffraction

3.2.1 Basic Principles of Neutron Diffraction

The SC research comprises many biophysical approaches such as Fourier transform infrared spectroscopy, differential scanning calorimetry, atomic force microscopy or nuclear magnetic resonance spectroscopy. Among those the scattering techniques X-ray and especially neutron diffraction are very potent methods to investigate the structure of isolated SC (Bouwstra et al. 1991) as well as SC model membranes constructed from extracted and synthetically derived SC lipids (Bouwstra et al. 1991, 1996, 1998; Friberg and Osborne 1987; Kuempel et al. 1998; McIntosh
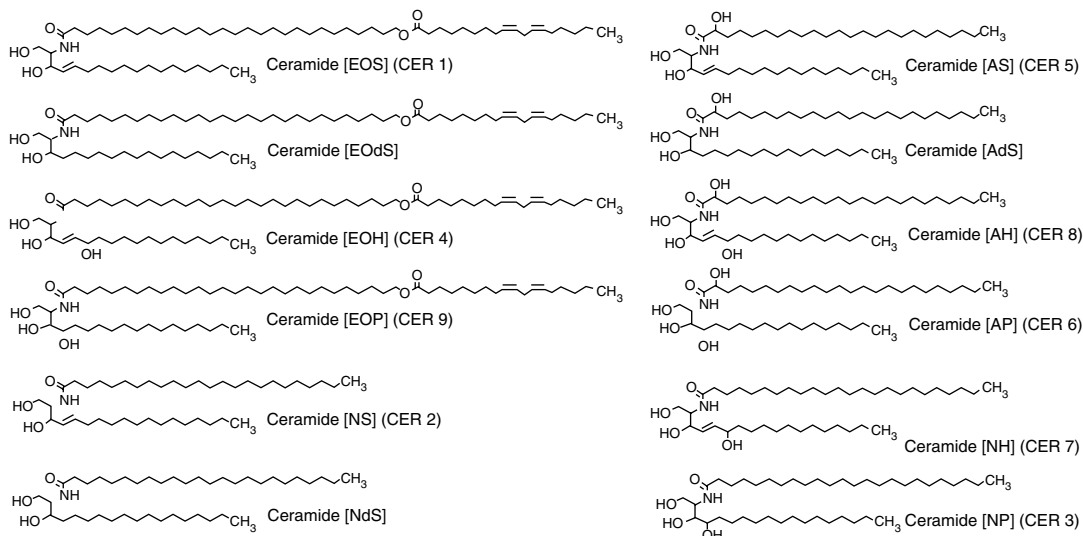
Fig. 3.1 Chemical structures of the ceramides found in the human stratum corneum. *S* Sphingosine, *P* Phytosphingosine, *H* 6-Hydroxysphingosine, *N* non-hydroxy fatty acid, *A* alpha-hydroxy fatty acid, *O* ω-hydroxy fatty acid, *E* esterified, *D* dihydro. In addition the old nomenclature according to the mobility of the CER in the thin layer chromatography was included for clarification

2003; McIntosh et al. 1996). Both neutron and X-ray diffraction are similar techniques, with the exception of the irradiation source. While X-rays primarily interact with the electrons of an atom, the interaction of neutrons with the atomic nucleus is short-ranged. To explain the several advantages of neutron over X-ray diffraction a brief explanation of these methods is necessary.

The technique of neutron diffraction is a versatile method to study the structure and dynamics, which specifically applies to biological samples. Due to their specific properties, neutrons may provide structural insights that are hardly obtained by other techniques, e.g., X-ray or light scattering. As non-charged particles, neutrons are enabled to penetrate matter deeply due to the small probability of interaction (Harroun et al. 2006). In contrast to X-rays, which are scattered by the electron cloud, neutrons interact with the atomic nucleus and are scattered isotropically (Dachs 1978). Hence, while the ability of elements to scatter X-rays increases with the atomic number throughout the periodic table of elements, such a correlation does not exist for neutrons (Cantor and Schimmel 1980). Particularly hydrogen, a light atom that is almost invisible for X-rays, is a strong scatterer for neutrons (see Fig. 3.2).

This makes neutron diffraction a particular valuable instrument to investigate structural and dynamic features especially in biological samples, which are rich in hydrogen. Moreover, neutrons show isotope sensitivity, i.e., even different isotopes of one element may have different scattering power for neutrons, for which hydrogen (1H) and deuterium (2H, D) are the most prominent examples (see Fig. 3.2) (Dachs 1978). The possibility to distinguish between components differing in their ability to scatter neutrons in one single sample, the so-called neutron contrast, is of great advantage for the study of biological systems like lipids and proteins (Büldt et al. 1978; Gutberlet et al. 2001; Tomita et al. 1999).

In a typical scattering experiment, a well-collimated neutron beam with a defined wavelength λ irradiates a sample, whereby the neutrons are scattered in all directions depending on the interactions between the sample material and the neutrons. The incoming neutrons interact with the sample and thereby experience a change in their momentum, which appears as a change of neutron direction and/or velocity. Consequently, monitoring the alterations of the neutron's momentum provides information regarding the
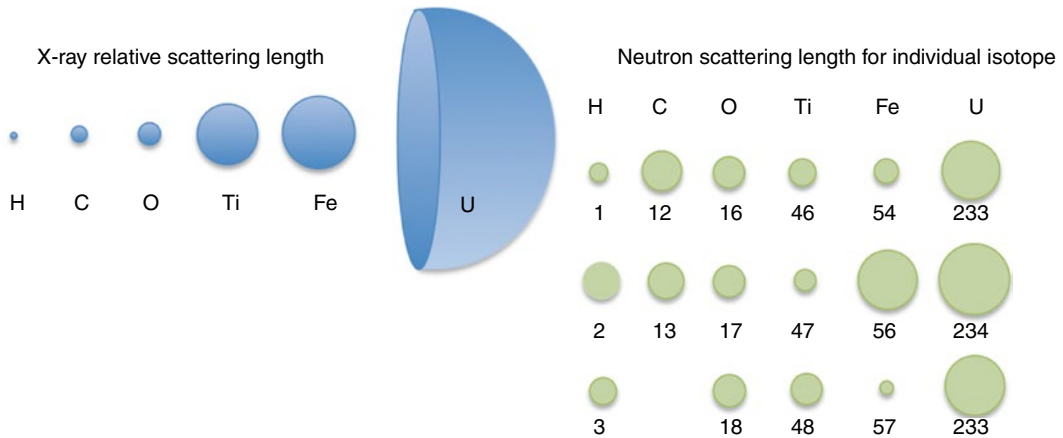
Fig. 3.2 Schematic comparison of the X-ray relative scattering lengths and neutron scattering lengths of different elements and their isotopes

structure and dynamics of the sample matter. To describe the change in momentum, the so-called momentum transfer vector, or *scattering vector* $\vec{Q}$, was introduced and is defined as the difference between incoming $\vec{k}_i$ and scattered $\vec{k}_s$ wave vectors $\vec{Q} = \vec{k}_i - \vec{k}_s$. In addition to a change in direction, the magnitude of $\vec{k}$ can also change as energy is transferred between incident neutrons and sample. When no energy is conveyed, the scattering process is considered to be totally elastic; therefore, $\vec{k}_i$ has to be equal to $\vec{k}_s$. Taking this in account, the scattering vector $\vec{Q}$ can be evaluated as $\vec{Q} = 2\vec{k}_i \cdot \sin\theta$, including the Bragg angle, which in case of crystalline and lamellar material appears at $\vec{Q}$ values equivalent to the

reciprocal spacing of the lattice: $\left|\vec{Q}\right| = \dfrac{2\pi}{d}$, where

by d denotes the characteristic spacing of a set of crystal planes. The complete Bragg formula $\lambda = 2d/\sin\theta$ can be received when the wave vector $\vec{k}_i$ is appropriately substituted with $\vec{k}_i = 2\pi / \lambda$.

Diffraction can be considered as a special type of scattering, whereby an organized structure such as a crystal or a lamellar arrangement is analyzed. According to Bragg's law, the incident beams are diffracted at a defined angle 2θ, and due to the interference between the waves, scattered from the parallel planes, diffraction occurs as depicted in Fig. 3.3.

The neutron scattering experiment now measures the scattering intensity I as a function of the scattering direction; the interpretation of the data offers information about the structure of the analyzed sample.

3.2.2 Investigation of Stratum Corneum Lipid Model Membranes with Neutron Diffraction

The initial biological materials, analyzed with neutron diffraction, were phospholipids due to the ability to form stable and highly organized multilamellar lipid bilayers necessary for neutron diffraction experiments. In recent years this technique has also been successfully introduced into the elucidation of the structural arrangement of the stratum corneum lipids. The application of neutron diffraction offers new possibilities to investigate the nanostructure of SC lipid systems and especially to gain information about the impact of the different CER subspecies as shown by Charalambopoulou and coworkers on fully hydrated human SC (Charalambopoulou et al. 2002) and by Kiselev et al. on well-defined SC lipid model membranes (Kiselev et al. 2005).

3.2.2.1 Evaluation of the Neutron Diffraction Data

As mentioned above, the scattering process is assumed as an elastic event with no energy transfer taking place. Consequently, the scattering
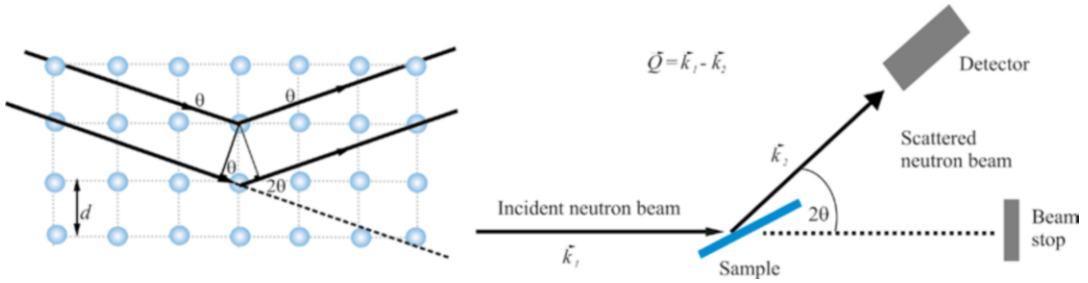
Fig. 3.3 Schematic drawing of the scattering process from ordered material. (*Left*) Neutrons strike an array of atoms (*spheres*) from the left side and are scattered to the right. The planes of atoms are separated by the interplanar distance d. The angle θ to the plans of atoms of the incident and the scattered beam are identical. The path length difference between the waves interfering constructively is equal to $2d \sin \theta$. (*Right*) A typical experimental setup of a neutron diffraction experiment, whereby $\vec{k}_i$ designates the incoming wave vector, while $\vec{k}_s$ represents the scattered neutron wave vector

vector $\vec{Q}$ can be correlated to the scattering angle 2θ. Furthermore, the intensity of the scattered neutron is measured as a function of the scattering angle 2θ. As the Bragg condition is complied, the integrated intensities can be calculated by using Gaussian fits to the received Bragg reflections. In order to gain deeper insight into the nanostructural arrangement of the SC lipids, it is necessary to compute the absolute value of the structure factors F_h from the integrated peak intensities: $|F_H| = A_h(\theta) \cdot \sqrt{h \cdot I_h}$ with Lorentz correction h and absorption factor $A_h(\theta)$ (Franks and Lieb 1979). The structure factor F_h serves as a mathematical description in which mode the incoming neutron wave is scattered by the investigated material (Franks and Lieb 1979; Nagle and Tristram-Nagle 2000a, b). The SC lipid multilamellar layers are composed of numerous bimolecular lipid membranes, which in other terms can be described as two equal monolayers facing each other. Such stacks of lipid layers are considered centrosymmetric for the neutron diffraction experiment, which allows for the construction of the neutron scattering length density (NSLD) profile $\rho_s(x)$ across the bilayer as Fourier transform

$$\rho_s(x) = \frac{2}{d} \sum_{h=1}^{h_{max}} F_h \cdot \left(\frac{2 \cdot \pi \cdot x}{d} \right)$$

(Nagle and Tristram-Nagle 2000b). In order to calculate the NSLD profile, it is essential to define the sign of the structure factor F_h. This can be easily done by variation of the D_2O/H_2O ratio in the sur-

rounding atmosphere, the so-called contrast variation (Wiener and White 1991), assuming that water can penetrate between the bilayer sheets (Franks and Lieb 1979; Worcester 1976). It was shown for such symmetrical and hydrated bilayers that the phase problem of F_hs simplifies to the determination of the sign of + or – (Franks and Lieb 1979) and can be derived from the slope of the correlation of F_h against the D_2O content in water vapor as shown in Fig. 3.4.

The NSLD profile offers detailed information about the nanostructure of the investigated lipid membrane and can also contribute to assign the position and orientation of the bilayer constituents. Furthermore, the evaluation of the NSLD profile allows for determining specific membrane regions such as the polar head groups, CH_3 groups, hydrocarbon chain region, and the region of cholesterol location (Kiselev et al. 2005). Next to the assignment of the position of these groups in the lipid bilayer membrane, the determination of parameters such as the region of polar head group or thickness of the intermembrane space further improves and intensifies the knowledge about such SC lipid organization.

3.2.3 Advantages and Disadvantages of Neutron Diffraction

As up to now a clear and detailed picture of the organization of the SC lipid matrix on a molecu-
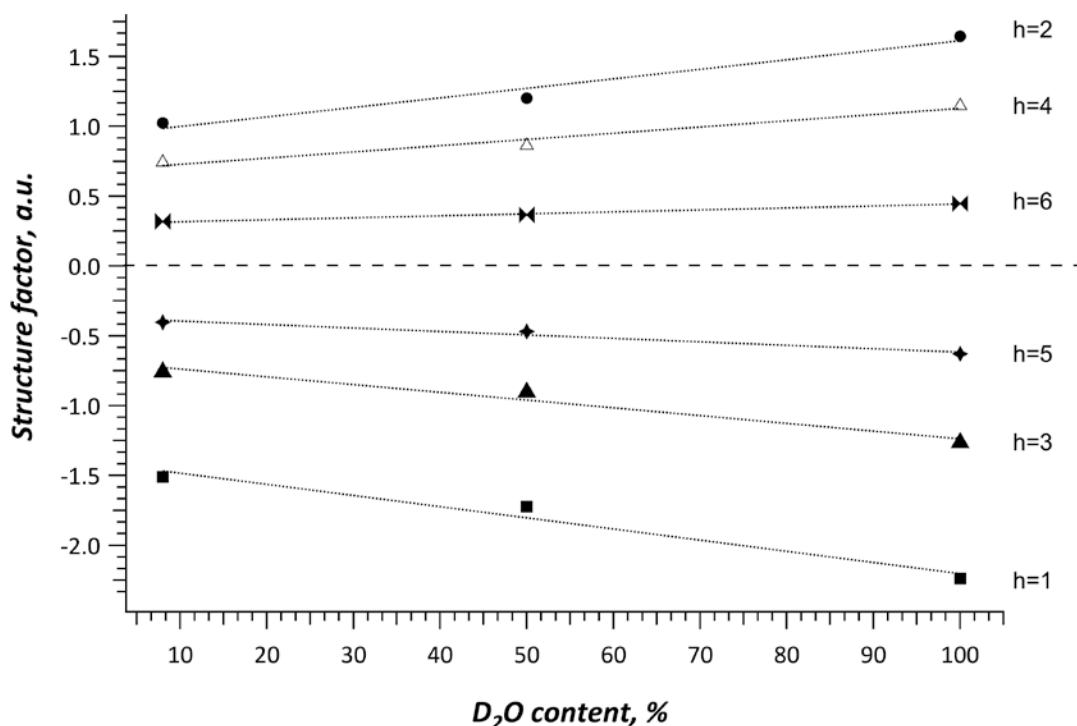
Fig. 3.4 Illustration of the dependency of the membrane structure factor F_h of the orders h = 1, 2, 3, 4 and 5 on the D_2O content on the water vapor a SC lipid model system

lar scale has not been elucidated, it is of supreme importance to comprehend the mode of action of the different SC lipid classes and particular the impact of the different ceramide subspecies. For the investigation of the driving forces and mechanisms that govern the self-assembling process of such lipid layers, the native SC lipid membranes are too complex objects to probe, especially with neutron diffraction. Consequently, for such an approach, model membranes will be the objects of choice. Moreover, issues due to the variability of the native lipids, for example, the variability in the head group architecture, can be overcome.

Neutrons as irradiation source are non-charged particles; they have only small interaction potential with matter, which enables a deep penetration into the studied material. This makes this method particularly suitable for biological issues such as the investigation of the structural arrangement of the SC lipids. In addition, as mentioned before the neutrons are scattered differently by different isotopes of the same element

(see Fig. 3.2). This special feature renders the possibility of the contrast variation as described before. In the same line, there is another distinct advantage of the neutron diffraction technique, which is the possibility of specific deuteration, as the coherent scattering length b_{coh} (the scattering ability) of hydrogen (^1H) and its isotope deuterium (^2H) differs significantly ($b_{coh}(^1H) = -3.741$ fm, $b_{coh}(^2H) = 6.671$ fm). Accordingly, hydrogen atoms in a lipid molecule can be specifically substituted by deuterium, which does not alter the properties of the lipid molecule. When a partially deuterated lipid sample is compared to its protonated counterpart, it is possible to identify the exact position of the labeled group within the lipid membrane (see Fig. 3.5). This is a distinct advantage of neutron diffraction over X-ray diffraction, which does not allow for such localization. As the SC lipid molecules are rich in hydrogen atoms, there is a variety of substitution positions, which then permit to make distinction between different conformational states of the studied lipid species. This feature is of high inter-
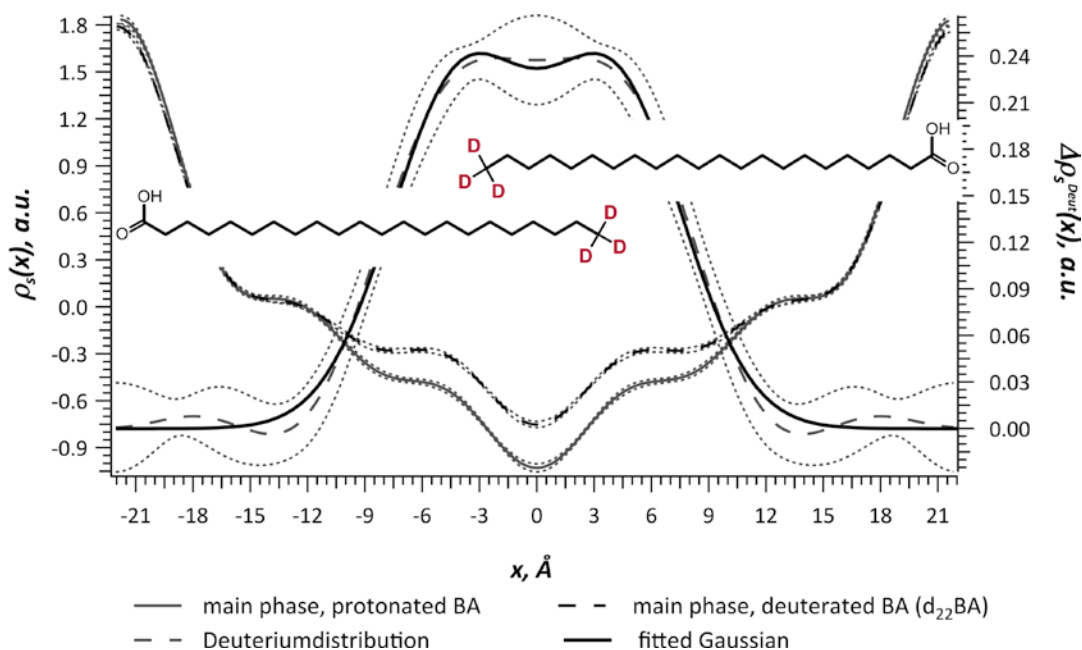
Fig. 3.5 Example of the localization of partially deuterated behenic acid (BA) molecules ($d_{22}BA$) in a SC lipid model membrane composed of ceramide [AP], cholesterol, $d_{22}BA$ and cholesterol sulfate. The neutron scattering length density (NSLD) profiles display the comparison of the sample membrane containing either deuterated (*dashed line*) or protonated BA (*solid line*). *Dotted lines*: corresponding errors, *Long dash*: difference NSLD profile, *Fat solid line*: fit of the difference NSLD profile by two Gaussian functions (deuterium distribution). All measurements were carried out at 57 % relative humidity, at 8 % D_2O in water vapor and T = 20 °C

est, especially for the investigation of SC lipids, as it is known for CER to exhibit different conformational states (Dahlen and Pascher 1972, 1979; Raudenkolb et al. 2003a, b, 2005).

The disadvantages are the limiting factors for application of the neutron diffraction for exploration of the SC lipid matrix. When compared to X-rays the neutron fluxes are relatively small, which necessitates a much longer experimental timescale and a higher amount of lipid material to achieve a reasonable signal-to-noise ratio. Furthermore, when native SC is probed with neutron diffraction, this yields to only one or two diffraction orders, which are not sufficient for the analysis of the NSLD profile (Charalambopoulou et al. 2002). Consequently only SC lipid model systems can be studied.

Another drawback of the neutron diffraction technique is its availability, as there exist only a few neutron facilities at which such an experiment can be carried out (e.g., Helmholtz Centre Berlin for Material and Energy (HZB) and Institut Laue-Langevin (ILL), Grenoble, France).

3.2.4 X-Ray Diffraction for the Investigation of the Stratum Corneum Lipids

As mentioned before, X-ray diffraction has been widely used for the investigation of the structural arrangement of the SC lipids. So Hatta and coworkers could establish the impact of ethanol on the lipid membranes. They discovered by X-ray diffraction, that lipid compounds can be extracted and even recrystallized as well (Hatta et al. 2001). The investigations of Kessner et al. could establish by X-rays that the phase behavior of the long-chain CERs is effected by their long acyl rests (Kessner et al. 2010).

Compared to other scattering techniques, it has a variety of advantages. In contrast to the above-described neutron diffraction technique, X-rays are scattered by the electrons surrounding the atomic nuclei. This results in peaks of high intensity and high resolution. Furthermore, many X-ray sources for such experiments are accessible.

Nevertheless, as described above the major drawback of the application of X-ray in the field of SC research is the low capability to depict light atoms such as hydrogen, which is one of the main components of a biological relevant material. Furthermore, as the number of electrons between different isotopes of the same element does not change, X-rays cannot distinguish isotopes. Its application as an irradiation source does not allow for the evaluation of the sign of the structure factor, which is essential in order to be able to calculate the scattering length density profile to gain deeper insight into the arrangement of the lipid bilayer. When the lamellar thickness of a lipid membrane is changed by way of varying the thickness of the water layer, it is possible to evaluate the sign of the structure factor and consequently calculate the electron density profile. However, it is well known that the repeat distances of SC lipid mixtures prepared from ceramides (CER), cholesterol (CHOL), and free fatty acids (FFAs) are very insensitive to hydration and that especially for the short periodicity phase (SPP), only a limited number of diffraction orders are obtained with X-ray diffraction. Therefore, again it is difficult to acquire an electron density profile by X-ray diffraction analysis.

3.3 ω-acyl Chain Ceramides and Their Influence on the Nanostructure of the Stratum Corneum Lipid Matrix

The lipids of the SC and particularly the ceramides (CER) are responsible to uphold the proper barrier function as pointed out in the introduction. The CER are a very heterogeneous group of sphingolipids (see Fig. 3.1), which can roughly be divided into two groups: (1) short-chain CER such as CER[AP] or CER[NP] and (2) the exceptionally long-chain ω-acyl CER such as CER[EOS] or CER[EOP]. So far, there has been a general consensus that especially the long-chain ω-acyl CER seem to be of particular relevance because of their unique structure.

Besides the assumed importance of long-chain ω-acyl CER in forming the so-called long-periodicity phase (LPP), their presence plays a key role with regard to some skin diseases. For atopic dermatitis there was found a decrease especially in the CER[EOS] content as proposed by Yamamoto and coworkers (Yamamoto et al. 1991), whereas psoriatic skin among others is thought to be caused by an increase in the CER[EOS] amount (Motta et al. 1994).

3.3.1 Physicochemical Aspects

In addition to the amidation of the sphingosine backbone, the ω-hydroxylated fatty acid is at its ω-position mainly esterified with a linoleic acid (EO) (Coderch et al. 2003). Nevertheless, Hinder and coworkers identified for CER [EOS] different amid-bound fatty acids with chain lengths varying from 17 to 22 carbon atoms (Hinder et al. 2011). The same chain length ranging was found for the sphingosine part. Therefore, it was concluded that not only linoleic acid as fatty acid compound is esterified to the sphingosine backbone. Subsequently, the influence of these different chain lengths was studied by de Sousa Neto et al. with small-angle X-ray scattering and Fourier transform infrared spectroscopy (de Sousa Neto et al. 2011). Their results show an important influence of chain length on the lipid organization. Whereas linoleate- and oleate-linked fatty acid CER[EOS] showed both the formation of the LPP and SPP, the stearate-linked variety did not form the LPP. Hence, unsaturated amid-bound fatty acids seem to be crucial for the formation of the LPP.

Due to the high mobility of the exceptionally long-chain ω-acyl residue, these CER form less ordered structures than it is known for short-chain CER (Raudenkolb 2002). Additionally, the melting points being 86 °C for CER[EOS] and above 100 °C for CER[EOP], respectively, hardly differ from those found for short-chain CER as stated by Kessner and coworkers (Kessner et al. 2010). The discrepancy in melting points of both ω-acyl chain CER was argued to be due to the more polar head group structure of CER[EOP] (2 OH groups for CER[EOS] versus 3 OH groups for CER[EOP]), which enables this CER to create more hydrogen bonds. In contrast to their expectations, Kessner and coworkers could additionally ascertain that the ther-
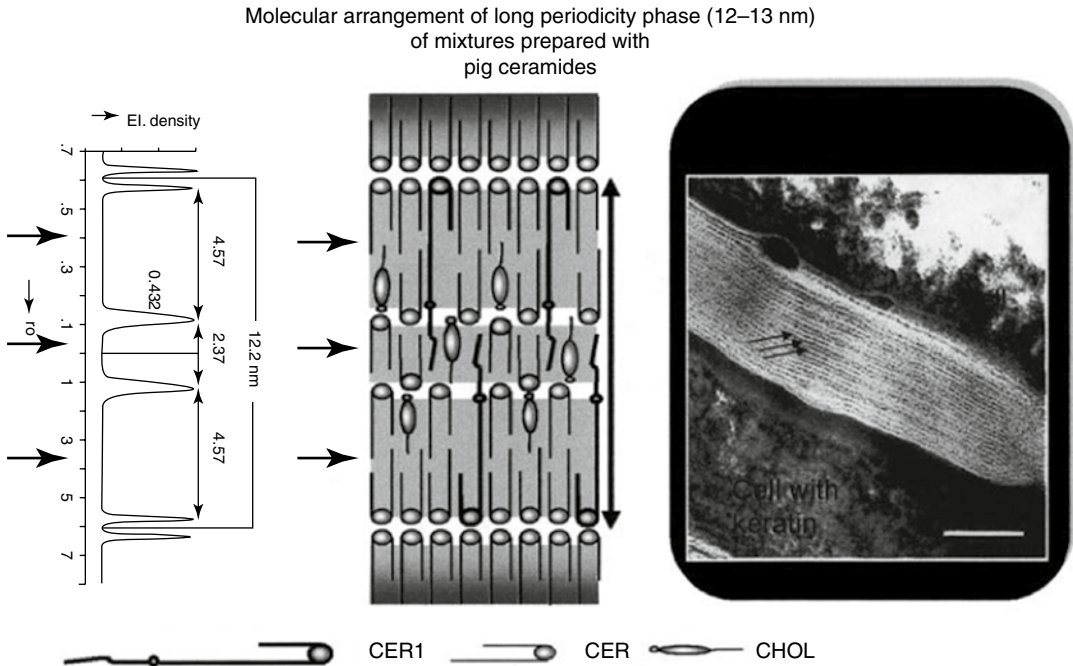
Fig. 3.6 Schematic presentation of the molecular arrangement of the long-periodicity phase (LPP). Reprinted from Bouwstra et al. (2001a) with permission from Karger Publisher

motropic phase behavior of these CER is reversible and the melting process does not induce major modifications of the lipids (Kessner et al. 2010). This is in line with other discoveries, which found the polar head group architecture to be responsible for polymorphism (Raudenkolb et al. 2003a, b, 2005).

3.3.2 Long-Chain ω-acyl Ceramides Studied Using Native Stratum Corneum

As there is a high demand to comprehend the structural arrangement of the different components of the SC lipid, especially, the long-chain CER were supposed to be of great influence. Consequently, the focus of many researchers was first placed on these exceptionally long-chain ω-acyl CER with their extraordinary characteristics concerning SC lipid organization. For example, Bouwstra et al. stated the importance of CER[EOS] not only for the formation of the LPP but also for the formation of a liquid phase which enables molecules to permeate along the lipid layer (Bouwstra et al. 2002). In this context the same group analyzed

mixtures of CER, cholesterol (CHOL), and free fatty acids (FFAs) with regard to a diminishing content of CER[EOS] by X-ray and electron diffraction studies (Bouwstra et al. 2001a). According to their assumption, the fraction of lipids forming the LPP decreases by reducing the amount of CER[EOS]. Thus, they concluded that the presence of the long-chain ω-acyl CER is necessary for the formation of the LPP and subsequently for a proper barrier function of the SC lipid matrix. Resulting from different electron diffraction studies, the LPP is described as a trilamellar broad-narrow-broad arrangement of the SC lipids with a membrane thickness or repeat distance of 13 nm (Madison et al. 1987; White et al. 1988). Based on these insights Bouwstra et al. developed the sandwich model, depicted in Fig. 3.6. According to this model the liquid sublattice consists of CHOL and the linoleic acid residues of the long ω-acyl CER[EOS], [EOP], and [EOH], which are located in the center of this trilamellar structure and encompass nearly 3 nm of the total 13 nm thickness of the LPP. The adjacent crystalline phases with a broadness of 5 nm on either side are composed of long saturated hydro-

carbon chains of the CER and FFA (Bouwstra et al. 2001a). Except the research of McIntosh et al. (1996), in which isolated CER from native pig epidermis were employed, all studies mentioned above directly used native SC derived from a pig or mouse tissue for their investigations.

But as pig CER differ structurally from CER originated from human tissue, Bouwstra and coworkers compared their previous results of mixtures containing pig CER with those containing human CER (Bouwstra et al. 2001b). Similar to pig CER/CHOL mixtures, human CER/CHOL mixtures showed the formation of the LPP with the difference, that by addition of FFA the LPP disappeared and has been replaced by a short periodicity phase (SPP) (Bouwstra et al. 2001b). Contrary to these findings various work groups could not detect an LPP by cryoelectron microscopy (Al-Amoudi et al. 2005; Pfeiffer et al. 2000) and X-ray diffraction (Garson et al. 1991) in human SC. They explained the discovery of the LPP in former researches as an artifact due to the fixation with Ruthenium tetroxide. Ruthenium tetroxide is necessary for the electron diffraction and might yield to the misinterpretation of the received data. However, the fixation problem does not account for the X-ray diffraction results.

3.3.3 Synthetically Constructed Long-Chain ω-acyl Ceramides

There are several disadvantages when native SC lipids are used. For instance, the variability in chain length of either the FFA or the CER-bound fatty acids and differences in the CER head group architecture (see Fig. 3.1) can circumvent the assignment of different characteristics to individual lipids, especially the CER subclasses. In recent years synthetically constructed CER with defined chemical structures have been introduced into the SC lipid research, enabling a more reliable transduction of the physicochemical behavior to the structural characteristics of special CER.

This was taken into consideration by de Jager et al. (2004), who confirmed the existence of the LPP by investigating synthetic CER in mixtures with CHOL and FFA using small-angle X-ray dif-

fraction. Additionally, they concluded that there is a close connection with the formation of the LPP and the presence of CER[EOS]. They stated that, while partial replacement of CER[EOS] by CER[EOP] does not influence phase behavior, complete substitution leads to a phase separation of CER[EOP] and a reduction of the LPP.

Another study performed by Kessner and coworkers also employed synthetically derived CER and applied both X-ray diffraction and Fourier transform Raman spectroscopy in order to ascertain these findings. Contrary to the previously described investigation, the physicochemical behavior of only the synthetic long ω-acyl CER[EOS] and [EOP] (Kessner et al. 2010) was studied without FFA or CHOL. These investigations revealed remarkable insights in this regard. While CER[EOS] in dry state only arranges in a SPP, CER[EOP] already forms the LPP. It was deduced that the differences in the head group architectures are responsible as this is the only dissimilarity between both CER species. They argued that the additional hydroxyl group in CER[EOP] is responsible for more hydrogen bonds and therefore enables the formation of a high-ordered package preventing the ω-acyl chains extending into the adjacent bilayer. Once both CER are hydrated, they are able to form the LPP with a repeat distance of 12 nm (Kessner et al. 2010).

To further examine the significance of these findings for the arrangement of the SC lipids, model membranes containing synthetic long-chain ω-acyl CER, CHOL, and FFA were analyzed. Using X-ray diffraction, mixtures of different CER, CHOL, and the FFA palmitic acid (PA) in an equimolar ratio were studied by de Jager et al. (2003). In mixtures containing CER[EOS]/CHOL/PA no LPP could be detected, while the same mixture comprising additionally CER[NP] showed a clear LPP with a repeat distance of 11.6 nm. The authors concluded that not only the presence of one single CER subclass can induce the formation of the LPP but a mixture of particular CER (de Jager et al. 2003).

Subsequently, Kessner and coworkers analyzed lipid mixtures containing CER[EOS], CER[AP], and CHOL. They detected a lamellar membrane with a thickness of two opposing CER[AP] molecules of approximately 45 Å indi-

Fig. 3.7 Schematic presentation of the arrangement of CER[EOS] in the model matrix composed of CER[EOS]/CER[AP]/CHOL/BA (23/10/33/33, w/w) according to Schroeter et al. (2008)
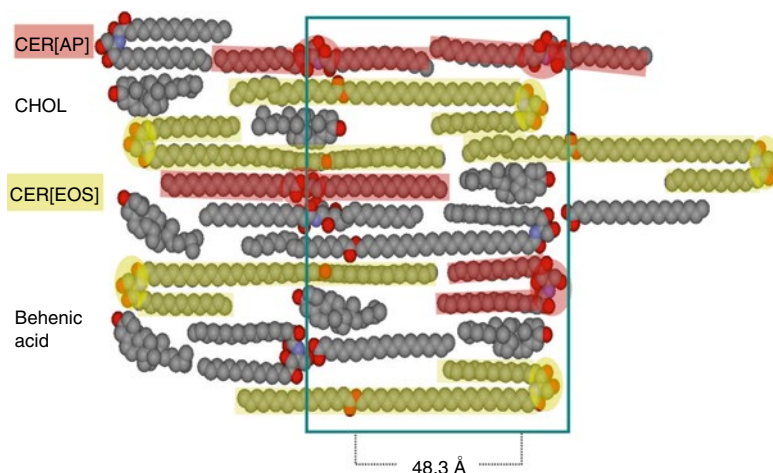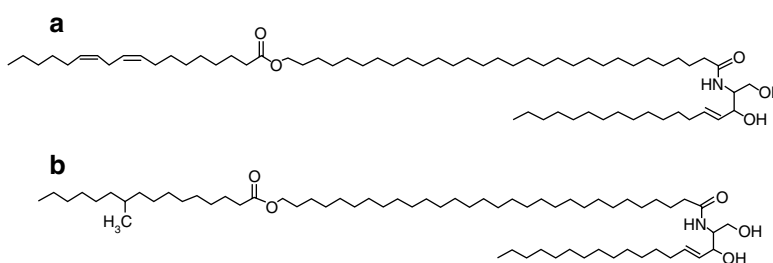

Fig. 3.8 Chemical structures of the native CER[EOS] specie (A) and the synthesized CER[EOS]_branched variety according to Engelbrecht et al. (2011)

cating that no LPP was formed (Kessner et al. 2008a). Even by adding of the FFA behenic acid (Schroeter et al. 2008), which was often reported to be required for the formation of the LPP (de Jager et al. 2003), only a slight increase of the repeat distance to 48 Å was perceived. Furthermore, from the neutron scattering length density profile, it was concluded that the long ω-acyl chain of CER[EOS] protrudes into the adjacent layer in order to fit into the membrane size created by CER[AP]. Consequently, CER[EOS] is positioned inside a phase with a short periodicity by spanning a bilayer and extending into adjacent layer (see Fig. 3.7).

It was concluded that the polar short-chain CER[AP] plays a key role in the formation of this lipid system. It dictates the arrangement of the other lipids within this mixture in a lamellar membrane, which covers the range of two opposing CER[AP] molecules. Consequently, the distinct head group polarity of CER[AP] exceeds the influence of the long ω-acyl chain of CER[EOS] (Kessner et al. 2008a; Schroeter

et al. 2008). In another approach by Engelbrecht and coworkers, an artificial derivative of CER[EOS], the so-called CER[EOS]_branched with a methyl-branched and saturated ω-acyl chain, was synthesized and investigated in a model membrane applying neutron diffraction (Engelbrecht et al. 2011) (see Fig. 3.8). This molecule is less sensitive to oxidative stress and therefore more stable and easier to handle as the native specie.

To assure the comparability of the native CER[EOS] and the artificial CER[EOS]_branched derivative both Fourier transform Raman spectroscopy and differential scanning calorimetry were carried out, with the outcome that both species show a comparable phase and chain packing behavior (Engelbrecht et al. 2011). In order to elucidate the arrangement of this CER[EOS] derivative with respect to the previously described findings, Engelbrecht et al. additionally studied a model membrane system composed of CER[EOS]_branched, CER[AP], CHOL, and behenic acid with neutron diffrac-

tion (Engelbrecht et al. 2011). They found that the synthetically derived CER[EOS]_branched is able to serve as an appropriate substitute for the native CER[EOS] in terms of lipid arrangement and architecture. Even this more stable and saturated acyl chain of CER[EOS]_branched did not induce a formation of the LPP in the presence of CER[AP], as stated above for the non-branched species in such mixtures. Again, the protruding influence of the more polar CER[AP] induces the formation of the SPP. To further verify their results, molecular dynamic simulation was performed and confirmed the lamellar arrangement of this model membrane (see Fig. 3.9).

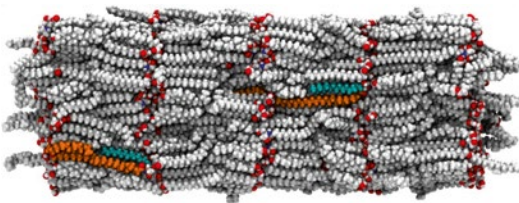Contrary to these findings there are the results from X-ray diffraction and FT-IR studies conducted by Groen et al. (2010). For mixtures containing CER[EOS], CHOL, and different FFA in an equimolar ratio, they could detect a 14.7 nm lamellar phase. This very long repeat distance was discussed to result from two opposing CER[EOS] molecules with interdigitating linoleate residues. Accordingly they proposed a model arrangement in which the lamellae are divided into three different lipid layers referred to as (A) (containing the linoleate residues of CER[EOS]), (B) (composing CHOL and CER[EOS]-ω-bound fatty acids), and (C) (buildup of sphingosine residues and FFA) as depicted in Fig. 3.10. Although a long 14.7 nm lamellar phase could be observed, the LPP with a repeat distance of 13 nm was not detected.

Concluding, it has to be stated that the role of long-chain ω-acyl CER both in context with the formation of the LPP or in terms of skin diseases is not completely elucidated and still debated vigorously. Therefore, these CER are still a subject of great interest in SC lipid research.

Fig. 3.9 Snapshot from molecular dynamic simulation of the lipid system consisting of CER[EOS]_branched/ CER[AP]/behenic acid/CHOL (23/10/ 33/33 m/m) and H₂O. Color code: *orange*: CER[EOS]_branched, *blue* CER[AP]. Modified according to Engelbrecht et al. (2011)

3.4 Effect of Short-Chain Ceramides to the Structural Organization of Stratum Corneum Lipids

As outlined previously, the heterogeneous class of CER can be generally separated into two major subclasses: the very long-chain ω-acyl CER like

Fig. 3.10 Model calculations of the neutron SLD profile of a SC lipid system composed of CER[AP], CHOL, behenic acid (BA), and cholesterol sulfate modified according to Ruettinger et al. (2008). The fitted curves for each group are: polar head groups (*blue dash*), CH₂-groups (*green*), CH₃-groups (*orange*), cholesterol (*red*)
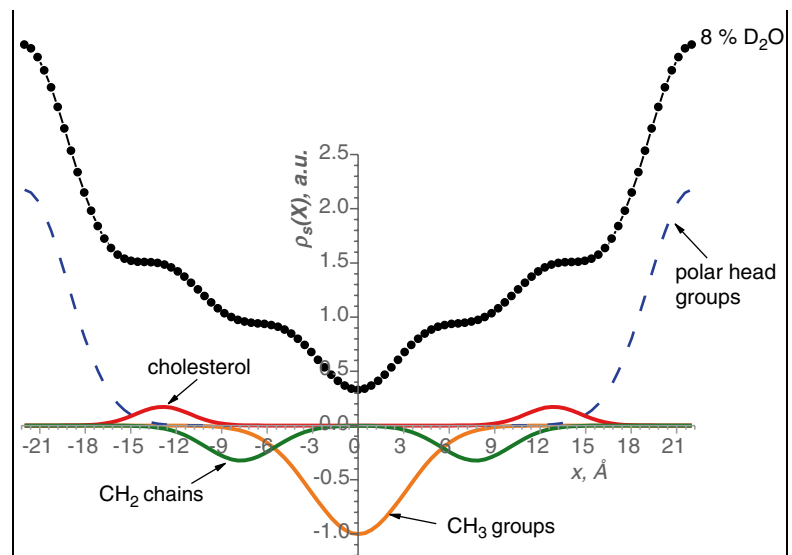
CER[EOS] or [EOP] and the short-chain CER, which can further be divided into the phytosphingosine type such as CER[AP] or CER[NP] and the sphingosine-type CER such as CER[AS] or CER[NS]. Furthermore, both subclasses are known to exhibit a broad distribution of their alkyl chain length, which is necessary for their proper functionality of the SC lipid matrix (Norlen 2001). During the last years, especially the short-chain CER of the phytosphingosine variety have gained in interest in the SC lipid research, as specific, their role for a proper barrier function has not been fully elucidated up to date. In order to evaluate the specific function of each CER subclass nowadays, well-defined model systems are investigated using different techniques.

The various experimental techniques such as X-ray diffraction, vibrational spectroscopy, or differential scanning calorimetry (DSC) to characterize the thermotropic and/or lyotropic properties of the ceramides as bulk substance and in different mixtures have been extensively reviewed before (Kessner et al. 2008c; Wartewig and Neubert 2007). In order to understand the impact of different CER species for the formation of the SC lipid matrix, the analysis of the CER as bulk material and then consequently in mixtures with other SC lipids is mandatory for the interpretation of the behavior in the complex multicomponent SC lipid membranes.

3.4.1 Elucidation of the Nanostructure of Stratum Corneum Lipid Models Based on CER[AP] or CER[NP]

As a first step to investigate the influences of different short-chain CER, Kiselev and coworkers prepared a SC lipid model membrane composed of CER[AP], cholesterol (CHOL), the free fatty acid (FFA) palmitic acid and cholesterol sulfate as oriented multilamellar membrane and investigated it with neutron diffraction (Kiselev et al. 2005). They showed by determining the internal membrane nanostructure and the water distribution across the bilayer, that such model membrane exhibits very low hydration, with a water layer

thickness of about 1 Å at full hydration. From the neutron scattering length density (NSLD) profile, they further derived information about the position of the molecular groups of the lipids within the lipid bilayer. This was achieved by fitting the NSLD profile with Gaussian functions, which resemble the position of the polar head groups, the CH_3 group, the hydrocarbon chain region, and the region of cholesterol location, respectively (see Fig. 3.10). Furthermore, they established that a decrease in the amount of CHOL in the model system correlates with an increase in the membrane thickness (Kiselev et al. 2005).

In order to identify the exact position of the CHOL molecules in this model membrane based on CER[AP], Kessner et al. employed two partially deuterated CHOL derivatives (Kessner et al. 2008b). From the neutron scattering length density (NSLD) profiles, they concluded that the CHOL molecules are immersed in the hydrocarbon chain region of the membrane bilayer, with the isopropyl residue positioned in the center of the membrane as depicted in Fig. 3.11.

As the interaction of the different lipid species of the SC matrix is of high interest, the influence of the FFA chain length to the above-described model membrane based on CER[AP], CHOL, and FFA was investigated also applying neutron diffraction (Ruettinger et al. 2008). In this study, within SC lipid model membranes, only the FFA chain length (C18:0 stearic acid, C22:0 behenic acid, C24:0 lignoceric acid, C26:0 hexacosanoic acid) was varied and the results were compared to each other. The membrane thickness for all investigated model systems was found to be in the range of two opposing CER[AP] molecules. An increase of the FFA chain length did not cause an alteration of the internal nanostructure but led to a slight decrease in the membrane thickness, causing a partial interdigitation of the longer chained FFA. The reason for the unexpected result was placed on the presence of the polar short-chain CER[AP]. This molecule establishes a tight hydrogen bond network between the adjacent bilayers due to its four OH groups. Thus, the CER forces the long-chain FFA to incorporate into the unchanged spacing of the bilayer, thereby obligating the FFA to protrude partly through opposing leaflet as represented in Fig. 3.12.

Fig. 3.11 Difference or deuterium distribution profile of the SC lipid model membrane derived from the difference between NSLD profile containing the deuterated CHOL derivative and the profile containing the protonated specie. Reprinted from Kessner et al. (2008b) with permission from Springer
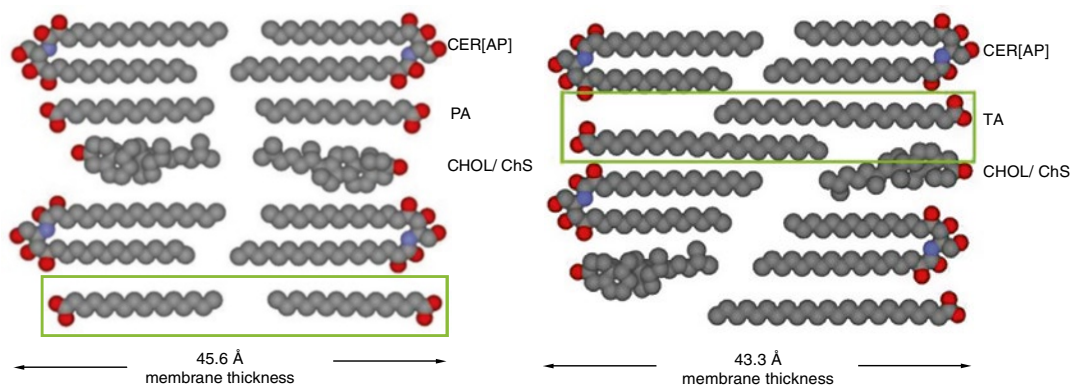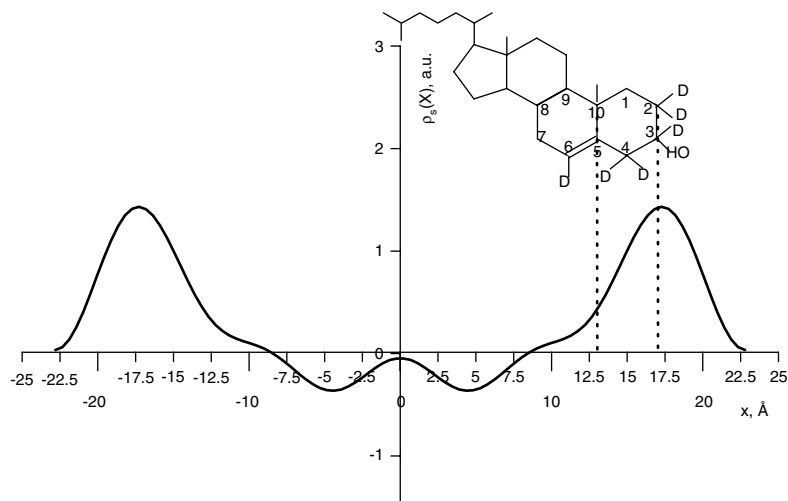

Fig. 3.12 Schematic presentation of the structural assembly of the SC model matrix based on CER[AP] according to Ruettinger et al. (2008). To demonstrate the influe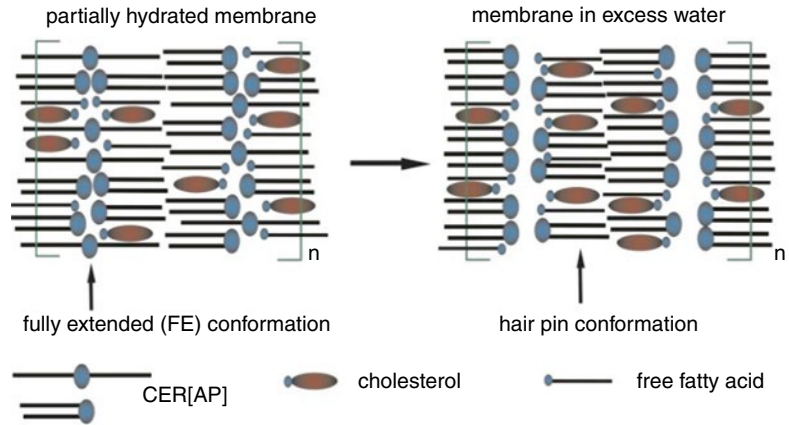nce of the longer chained FFA a model for the mem-brane containing palmitic acid (*left*) is compared to the matrix including tetracosanoic acid (*right*). *CER[AP]* ceramide [AP], *CHOL* cholesterol, *PA* palmitic acid, *TA* tetracosanoic acid

Consequently, CER[AP] creates a super-stable structure, which is not influenced by the alteration of the FFA chain length. The resulting free space due to the interdigitation of the FFA can only be compensated by pulling the membrane together, hence, the slight decrease in the membrane repeat distance. Additionally, the experiments revealed that the longer-chained FFA tends to separate in an FFA-rich phase. It was reasoned that the elongation of the chain length of the FFA decreases the solubility of the FFA in the SC model membrane based on the short-chain CER[AP] (Ruettinger et al. 2008). To verify the interdigitation of the FFA in the CER[AP]-based SC lipid model membrane, the

same group employed the partially deuterated FFA behenic-22,22,22-d3-acid and cerotic-12,12,13,13-d4-acid (Schroeter et al. 2009). The results from the neutron diffraction study provided the direct experimental evidence concerning the localization of the FFA in this SC lipid model system. Both the interdigitation and the presence of the FFA-rich phase could be proven by this method.

As mentioned earlier, such SC lipid membranes show very small head group hydration. Therefore, Ryabova and coworkers investigated the kinetics of the exchange of water in CER[AP]-based SC lipid model membranes with real-time neutron diffraction (Ryabova

Fig. 3.13 Schematic presentation of the armature reinforcement model and transformation of SC lipid membrane from partly hydrated to fully hydrated state by the excess of water modified according to Kiselev (2007)

Fig. 3.14 Conformational states of the short-chain CER

et al. 2009). The study revealed that the kinetic hydration comprises a fast initial segment, which is followed by two slow stages. By increasing the temperature to 57 °C, this process was significantly faster in its initial phase. Furthermore, they found that an irreversible phase separation at this temperature and low hydration level occurs, whereby they argued that the FFA separate. In a further investigation the same group studied the influence of both a realistic FFA mixture and cholesterol sulfate (ChS) to the structure of the above-described SC lipid model membrane based on CER[AP] (Ryabova et al. 2010). Again, as described by Ruettinger et al. (2008), not even a mixture of different FFA affects the nanostructure of this model system. Once more, the FFA needs to interdigitate in order to fit into the bilayer created by CER[AP]. Nevertheless, they found that their mixture containing six FFAs differing in chain length prevented the above-described FFA phase separation. Only the hydration behavior was altered due to the FFA mixture as Ryabova et al. discovered that the membrane swelling process was accelerated at low hydration levels, which was attributed to the less dense bilayer packing due to the interdigitation of the FFA (Ryabova et al. 2010). In the same study, no alteration of the rate of hydration was observed for the complete substitution of ChS by CHOL. However, the absence of ChS caused a phase separation, which was attributed to the missing sulfate group of ChS. As the sulfate group is negatively charged, it can increase the molecular area per lipid, which subsequently reduces the den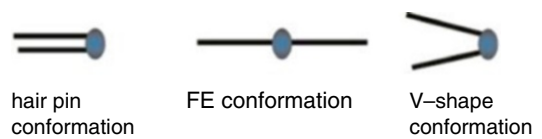sity of the lipid packing. This density reduction increases the mobility of the lipids, which further promotes the miscibility of the lipids. When, on the other hand, the amount of ChS was increased at the expense of CHOL, the swelling of the membrane increased. Ryabova et al. argued that the higher ability to form hydrogen bonds of ChS is responsible for this effect (Ryabova et al. 2010).

As described in the preceding chapter, the presence of CER[AP] in an SC lipid membrane composed also of CER[EOS], CHOL, and FFA prevents the formation of the LPP, as it forces the long ω-acyl chain of CER[EOS] to protrude through the complete bilayer into the adjacent layer (Engelbrecht et al. 2011; Kessner et al. 2008a; Schroeter et al. 2008). These experimental findings contributed to or are in accordance with the so-called armature reinforcement model, a theoretical model describing the molecular arrangement of these lipids (Kiselev 2007) (see Fig. 3.13).

Here, the polymorphism of the short-chain CER (Pascher 1976; Pascher and Sundell 1992; Raudenkolb et al. 2003a, b, 2005) is taken into account, as the role of the fully extended conformation is discussed for the arrangement of the lipids (Fig. 3.14). This model conception assumes that CER[AP] in its fully extended

conformation adopts a sort of anchor function due to the strong intermembrane attractions, in which it is able to restrain the other lipids inside the membrane and, respectively, forces their arrangement within the membrane constraints. Upon hydration, CER[AP] is capable to perform a chain-flip transition to the one-sided or hairpin conformation, which accounts for the alterations in the structure observed in the hydrated state (Kiselev et al. 2005).

Next to neutron diffraction, there is also the very powerful technique of neutron small angle scattering (SANS), which allows for the investigation of the structure of vesicular lipids in excess of water. With SANS nanostructural parameters such as size of the vesicle, thickness of a lipid bilayer, thickness of hydrophobic and hydrophilic regions, and number of water molecules can be directly determined (Kiselev et al. 2006). Applying these methods Zemlyanaya and coworkers (Zemlyanaya et al. 2008) investigated CER[AP]-based quaternary unilamellar vesicles. In their investigation they detected a short-range interaction between the vesicles specimen, which leads to the formation of clustered structures. Furthermore, with this study they confirmed the chain-flip transition of the CER[AP] molecules described above in the *armature reinforcement model*.

As CER[NP] is one of the most abundant CER of the SC (Masukawa et al. 2009), the focus was also placed on this molecule. Compared to the above-described CER[AP], this CER also belongs to the phytosphingosine subclass, but does not have the α-hydroxy group present in CER[AP]. Accordingly, the lamellar nanostructure of a SC lipid model membrane based on CER[NP] was investigated in an interdisciplinary approach using both neutron diffraction and 2H-NMR spectroscopy and then compared to the above-described CER[AP]-based SC lipid model systems by Engelbrecht and coworkers (Engelbrecht et al. 2012). The authors indicated that in the presence of this CER subspecies a highly ordered lipid lamellae is formed and phase separation occurred, which was even at high temperature in a densely packed and stable bilayer. Here, intra- and intermolecular head group interactions of CER[NP] prevent the hydration of the head group region. From the neutron diffraction data, it was proposed that CER[NP] exhibits a V-shaped conformation in both lamellar phases, but with the distinction that one phase is phase-separated CER[NP] as portrayed in Fig. 3.15, which was further corroborated by 2HNMR spectroscopy study.

Moreover, the model system based on CER[NP] a completely different diffraction pattern at higher temperature, when compared to the above-described CER[AP]-based lipid membranes. Thus, it was argued that the absence of just one OH group induces drastic structural alteration in the membrane arrangement.

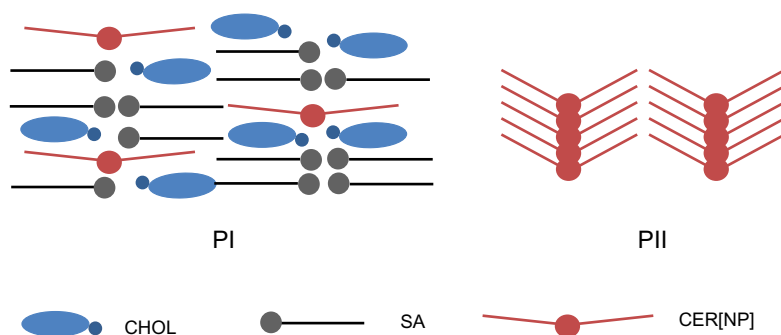**Fig. 3.15** Sketch of the assumed lamellar lipid assembly present in the phase-separated domains of PI and PII in the ternary SC lipid model membrane containing CER[NP], CHOL and SA at 80 °C and 99 % RH. While PII is constituted by crystalline CER[NP] showing a V-shaped conformation, PI is formed by CER[NP], SA and CHOL. Reproduced from Engelbrecht et al. (2012). with permission from The Royal Society of Chemistry

Fig. 3.16 Comparison of the Neutron scattering length density profile of the sample containing the protonated CER[NS] (*solid line*) and the deuterated variety (*dashed line*). Taken from Groen et al. (2011) with permission from Cell press
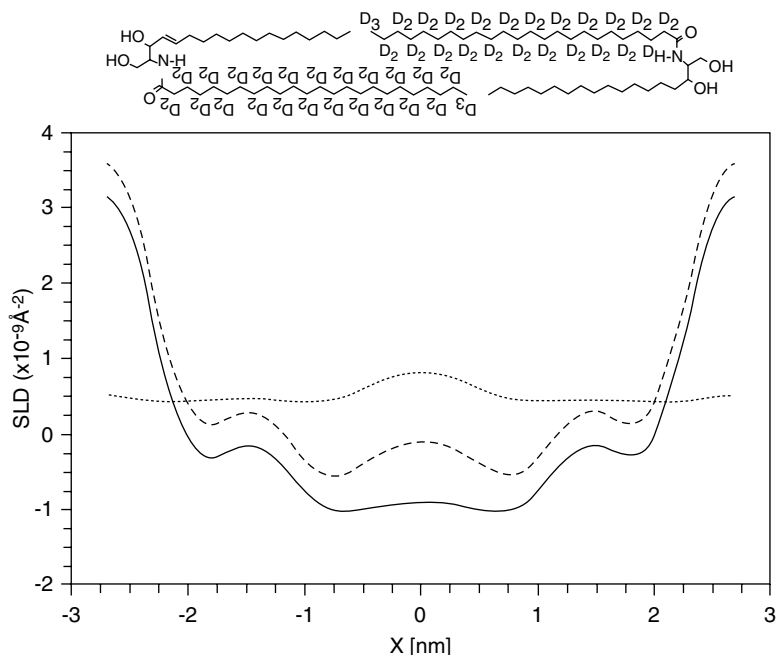
3.4.2 Investigating the Nanostructure of an Stratum Corneum Substitute

The above-portrayed investigations were mainly focused on the impact of *one* specific CER species in order to explicitly recognize the interaction occurring between the different lipids and identify the structure-function relationship of different CER subspecies. In another approach Groen and coworkers studied the nanostructure of SC lipid model membranes with neutron diffraction, which was composed of different CER species, CHOL, and FFA to closely mimic the SPP (Groen et al. 2011). In order to localize the CER, they applied a CER species (CER[NS]) with a perdeuterated acyl chain. In accordance with the finding described concerning the short-chain CER[AP], a bilayer arrangement with a membrane thickness in the range of two opposing CER molecules was detected. From the neutron scattering length density profile of the membrane containing the deuterated CER[NS] variety, they reasoned that the CER exhibits a symmetrical organization and excluded the asymmetric conformation of the CER inside the bilayer arrangement (Engelbrecht et al. 2012) as schematically displayed in Fig. 3.16.

However, as the acyl chain of CER[NS] is perdeuterated, only the presence of this chain can be deduced from the data. It is true that the chains need to be partially interdigitated in order to be in agreement with the neutron diffraction data. Nevertheless, another arrangement is possible whereby the CER molecules exhibit a fully extended conformation (see Fig. 3.14), the deuterated chains forming one leaflet, while the sphingosine backbone chain is pointed in the opposing direction.

Consequently, the drawback of the application of perdeuterated lipids in the neutron diffraction experiment is the fact that it does not yield to an unambiguous location of the labeled lipid species, and, furthermore, it does not give any information about the conformational state of the studied lipid.

3.5 Summary and Final Remarks

The intercellular lipid membranes of the SC are an excellent biological example for the relationship between the lipid composition, its physicochemical properties and biological function, as well as organization. To elucidate the special

assembly and the properties of the native SC lipid matrix is a very difficult task as the natural SC membranes are very complex. Therefore, in recent years the researches were primarily placed on the investigation of model systems in order to gain deeper insights into the driving forces of the lipid assembling process. Furthermore, not only model membranes are currently in the focus of different investigation but also rather simplistic, nonetheless realistic SC model membranes. As described, this offers the distinct benefit to analyze the different lipid species systematically. This approach is very important, as especially the impact of the various CER subclasses for the proper barrier function of the SC needs to be studied independently as shown for the very closely related CER[AP] and CER[NP].

So far a diversity of techniques have been introduced into this field, whereby neutron diffraction with its specific advantages seems to be the most promising one for the investigation of the nanostructure of the SC lipid matrix, as it enables the use of specifically labeled molecules. However, only a combination of different methods and approaches can provide a complete picture of the molecular arrangement of SC lipid matrix, as one technique alone can cover only a small field.

Up to date only a few CER subspecies have been investigated independently and are in parts debated controversially (see CER[EOS], for instance). Consequently, there is still a high demand to fully understand the impact of these lipids for a proper barrier function of the SC lipid matrix.

References

Al-Amoudi A, Dubochet J, Norlen L (2005) Nanostructure of the epidermal extracellular space as observed by cryo-electron microscopy of vitreous sections of human skin. J Invest Dermatol 124:764–777

Bouwstra JA, Gooris GS, van der Spek JA, Bras W (1991) Structural investigations of human stratum corneum by small-angle x-ray scattering. J Invest Dermatol 97:1005–1012

Bouwstra JA, Gooris GS, Cheng K, Weerheim A, Bras W, Ponec M (1996) Phase behavior of isolated skin lipids. J Lipid Res 37:999–1011

Bouwstra JA, Gooris GS, Dubbelaar FE, Weerheim AM, Ijzerman AP, Ponec M (1998) Role of ceramide 1 in the molecular organization of the stratum corneum lipids. J Lipid Res 39:186–196

Bouwstra J, Pilgram G, Gooris G, Koerten H, Ponec M (2001a) New aspects of the skin barrier organization. Skin Pharmacol Appl Skin Physiol 14(Suppl 1): 52–62

Bouwstra JA, Gooris GS, Dubbelaar FE, Ponec M (2001b) Phase behavior of lipid mixtures based on human ceramides: coexistence of crystalline and liquid phases. J Lipid Res 42:1759–1770

Bouwstra JA, Gooris GS, Dubbelaar FE, Ponec M (2002) Phase behavior of stratum corneum lipid mixtures based on human ceramides: the role of natural and synthetic ceramide 1. J Invest Dermatol 118:606–617

Büldt G, Gally HU, Seelig A, Seelig J, Zaccai G (1978) Neutron diffraction studies on selectively deuterated phospholipid bilayers. Nature 271:184

Cantor CR, Schimmel PR (1980) Biophysical chemistry: part II: techniques for the study of biological structure and function. Freeman, San Francisco

Charalambopoulou GC, Steriotis TA, Hauss T, Stefanopoulos KL, Stubos AK (2002) A neutron-diffraction study of the effect of hydration on stratum corneum structure. Appl Phys A 74:s1245–s1247

Coderch L, Lopez O, de la Maza A, Parra JL (2003) Ceramides and skin function. Am J Clin Dermatol 4:107–129

Dachs H (1978) Principles of neutron diffraction. In: Dachs H (ed) Neutron diffraction. Springer, Berlin, p 357

Dahlen B, Pascher I (1972) Molecular arrangements in sphingolipids - crystal-structure of N-tetracosanoylphytosphingosine. Acta Crystallogr B Struct B 28:2396

Dahlen B, Pascher I (1979) Molecular arrangements in sphingolipids – thermotropic phase-behavior of tetracosanoylphytosphingosine. Chem Phys Lipids 24:119–133

de Jager MW, Gooris GS, Dolbnya IP, Bras W, Ponec M, Bouwstra JA (2003) The phase behaviour of skin lipid mixtures based on synthetic ceramides. Chem Phys Lipids 124:123–134

de Jager M, Gooris G, Ponec M, Bouwstra J (2004) Acylceramide head group architecture affects lipid organization in synthetic ceramide mixtures. J Invest Dermatol 123:911–916

de Sousa Neto D, Gooris G, Bouwstra J (2011) Effect of the [omega]-acylceramides on the lipid organization of stratum corneum model membranes evaluated by X-ray diffraction and FTIR studies (Part I). Chem Phys Lipids 164(3):184–95

Engelbrecht T, Hauss T, Suss K, Vogel A, Roark M, Feller SE, Neubert RHH, Dobner B (2011) Characterisation of a new ceramide EOS species: synthesis and investigation of the thermotropic phase behaviour and influence on the bilayer architecture of stratum corneum lipid model membranes. Soft Matter 7:8998–9011

Engelbrecht TN, Schroeter A, Hauß T, Deme B, Scheidt HA, Huster D, Neubert RHH (2012) The impact of ceramides NP and AP on the nanostructure of stratum

corneum lipid bilayer. Part I: neutron diffraction and 2H NMR studies on multilamellar models based on ceramides with symmetric alkyl chain length distribution. Soft Matter 8:2599

Franks NP, Lieb WR (1979) The structure of lipid bilayers and the effects of general anaesthetics. An x-ray and neutron diffraction study. J Mol Biol 133:469–500

Friberg SE, Osborne DW (1987) Interaction of a model epidermal lipid with a vegetable oil adduct. J Dispers Sci Technol 8:249–258

Garson JC, Doucet J, Leveque JL, Tsoucaris G (1991) Oriented structure in human stratum corneum revealed by x-ray diffraction. J Invest Dermatol 96:43–49

Groen D, Gooris GS, Bouwstra JA (2010) Model membranes prepared with ceramide EOS, cholesterol and free fatty acids form a unique lamellar phase. Langmuir 26:4168–4175

Groen D, Gooris GS, Barlow DJ, Lawrence MJ, van Mechelen JB, Demé B, Bouwstra JA (2011) Disposition of ceramide in model lipid membranes determined by neutron diffraction. Biophys J 100:1481–1489

Gutberlet T, Heinemann U, Steiner M (2001) Protein crystallography with neutrons – status and perspectives. Acta Crystallogr D 57:349–354

Harroun TA, Wignall GD, Katsaras J (2006) Neutron scattering for biology. In: Fitter J, Gutberlet T, Katsaras J (eds) Neutron scattering in biology: techniques and applications. Springer, Berlin

Hatta I, Ohta N, Ban S, Tanaka H, Nakata S (2001) X-Ray diffraction study on ordered, disordered and reconstituted intercellular lipid lamellar structure in stratum corneum. Biophys Chem 89:239–242

Hinder A, Schmelzer CEH, Rawlings AV, Neubert RHH (2011) Investigation of the molecular structure of the human stratum corneum ceramides [NP] and [EOS] by mass spectrometry. Skin Pharmacol Physiol 24:127–135

Holleran WM, Man MQ, Gao WN, Menon GK, Elias PM, Feingold KR (1991) Sphingolipids are required for mammalian epidermal barrier function. Inhibition of sphingolipid synthesis delays barrier recovery after acute perturbation. J Clin Invest 88:1338–1345

Holleran WM, Takagi Y, Uchida Y (2006) Epidermal sphingolipids: metabolism, function, and roles in skin disorders. FEBS Lett 580:5466

Kessner D, Kiselev M, Dante S, Hauss T, Lersch P, Wartewig S, Neubert RHH (2008a) Arrangement of ceramide [EOS] in a stratum corneum lipid model matrix: new aspects revealed by neutron diffraction studies. Eur Biophys J Biophys 37:989–999

Kessner D, Kiselev MA, Hauss T, Dante S, Wartewig S, Neubert RHH (2008b) Localisation of partially deuterated cholesterol in quaternary SC lipid model membranes: a neutron diffraction study. Eur Biophys J Biophys 37:1051–1057

Kessner D, Ruettinger A, Kiselev MA, Wartewig S, Neubert RH (2008c) Properties of ceramides and their impact on the stratum corneum structure: part 2: stratum corneum lipid model systems. Skin Pharmacol Physiol 21:58–74

Kessner D, Brezesinski G, Funari SS, Dobner B, Neubert RHH (2010) Impact of the long chain [omega]-acylceramides on the stratum corneum lipid nanostructure. Part 1: thermotropic phase behaviour of CER[EOS] and CER[EOP] studied using x-ray powder diffraction and FT-raman spectroscopy. Chem Phys Lipids 163:42–50

Kiselev MA (2007) Conformation of ceramide 6 molecules and chain-flip transitions in the lipid matrix of the outermost layer of mammalian skin, the stratum corneum. Crystallogr Rep 52:525–528

Kiselev MA, Ryabova NY, Balagurov AM, Dante S, Hauss T, Zbytovska J, Wartewig S, Neubert RH (2005) New insights into the structure and hydration of a stratum corneum lipid model membrane by neutron diffraction. Eur Biophys J 34:1030–1040

Kiselev MA, Zemlyanaya EV, Aswal VK, Neubert RH (2006) What can we learn about the lipid vesicle structure from the small-angle neutron scattering experiment? Eur Biophys J 35:477–493

Kuempel D, Swartzendruber DC, Squier CA, Wertz PW (1998) In vitro reconstitution of stratum corneum lipid lamellae. Biochim Biophys Acta 1372:135–140

Madison KC, Swartzendruber DC, Wertz PW, Downing DT (1987) Presence of intact intercellular lipid lamellae in the upper layers of the stratum corneum. J Invest Dermatol 88:714–718

Masukawa Y, Narita H, Shimizu E, Kondo N, Sugai Y, Oba T, Homma R, Ishikawa J, Takagi Y, Kitahara T, Takema Y, Kita K (2008) Characterization of overall ceramide species in human stratum corneum. J Lipid Res 49:1466–1476

Masukawa Y, Narita H, Sato H, Naoe A, Kondo N, Sugai Y, Oba T, Homma R, Ishikawa J, Takagi Y, Kitahara T (2009) Comprehensive quantification of ceramide species in human stratum corneum. J Lipid Res 50:1708–1719

McIntosh TJ (2003) Organization of skin stratum corneum extracellular lamellae: diffraction evidence for asymmetric distribution of cholesterol. Biophys J 85:1675–1681

McIntosh TJ, Stewart ME, Downing DT (1996) X-ray diffraction analysis of isolated skin lipids: reconstitution of intercellular lipid domains. Biochemistry 35:3649–3653

Motta S, Monti M, Sesana S, Caputo R, Carelli S, Ghidoni R (1993) Ceramide composition of the psoriatic scale. Biochim Biophys Acta 1182:147–151

Motta S, Monti M, Sesana S, Mellesi L, Ghidoni R, Caputo R (1994) Abnormality of water barrier function in psoriasis. Role of ceramide fractions. Arch Dermatol 130:452–456

Nagle JF, Tristram-Nagle S (2000a) Lipid bilayer structure. Curr Opin Struct Biol 10:474–480

Nagle JF, Tristram-Nagle S (2000b) Structure of lipid bilayers. Biochim Biophys Acta 1469:159–195

Norlen L (2001) Skin barrier structure and function: the single gel phase model. J Invest Dermatol 117:830–836

Pascher I (1976) Molecular arrangements in sphingolipids conformation and hydrogen-bonding of ceramide and

their implication on membrane stability and permeability. Biochim Biophys Acta 455:433–451

Pascher I, Sundell S (1992) Molecular arrangements in sphingolipids: crystal structure of the ceramide N-(2d, 3d-dihydroxyoctadecanoyl)-phytosphingosine. Chem Phys Lipids 62:79–86

Pfeiffer S, Vielhaber G, Vietzke JP, Wittern KP, Hintze U, Wepf R (2000) High-pressure freezing provides new information on human epidermis: simultaneous protein antigen and lamellar lipid structure preservation. Study on human epidermis by cryoimmobilization. J Invest Dermatol 114:1030–1038

Raith K, Farwanah H, Wartewig S, Neubert RHH (2004) Progress in the analysis of stratum corneum ceramides. Eur J Lipid Sci Technol 106:561–571

Raudenkolb S (2002) Untersuchungen zur strukturellen und physikochemischen charakterisierung von stratum corneum lipiden und deren mischsystemen Institute of Pharmacy, vol PhD. Martin-Luther-Universität Halle-Wittenberg, Halle (Saale)

Raudenkolb S, Hubner W, Rettig W, Wartewig S, Neubert RH (2003a) Polymorphism of ceramide 3. Part 1: an investigation focused on the head group of N-octadecanoylphytosphingosine. Chem Phys Lipids 123:9–17

Raudenkolb S, Wartewig S, Neubert RH (2003b) Polymorphism of ceramide 3. Part 2: a vibrational spectroscopic and X-ray powder diffraction investigation of N-octadecanoyl phytosphingosine and the analogous specifically deuterated d(35) derivative. Chem Phys Lipids 124:89–101

Raudenkolb S, Wartewig S, Neubert RH (2005) Polymorphism of ceramide 6: a vibrational spectroscopic and x-ray powder diffraction investigation of the diastereomers of N-(alpha-hydroxyoctadecanoyl)-phytosphingosine. Chem Phys Lipids 133:89–102

Ruettinger A, Kiselev MA, Hauss T, Dante S, Balagurov AM, Neubert RH (2008) Fatty acid interdigitation in stratum corneum model membranes: a neutron diffraction study. Eur Biophys J 37:759–771

Ryabova N, Kiselev M, Balagurov A (2009) Transition processes in stratum corneum model lipid membranes with a mixture of free fatty acids. Biophysics 54:598–606

Ryabova NY, Kiselev MA, Dante S, Hauss T, Balagurov AM (2010) Investigation of stratum corneum lipid model membranes with free fatty acid composition by neutron diffraction. Eur Biophys J 39:1167–1176

Schroeter A, Engelbrecht T, Hauß T, Neubert RHH (2008) Role of ceramide [AP] and ceramide [EOS] in the structural assembly of stratum corneum model membrane. BENSC experimental reports. Helmholtz Zentrum Berlin für Materialien und Energie, Berlin

Schroeter A, Kiselev MA, Hauß T, Dante S, Neubert RHH (2009) Evidence of free fatty acid interdigitation in stratum corneum model membranes based on ceramide [AP] by deuterium labelling. BBA Biomembr 1788:2203

Tomita M, Hasegawa T, Tsukihara T, Miyajima S, Nagao M, Sato M (1999) Two concentric protein shell structure with spikes of silkworm Bombyx mori cytoplasmic polyhedrosis virus revealed by small-angle neutron scattering using the contrast variation method. J Biochem (Tokyo) 125:916–922

Wartewig S, Neubert RHH (2007) Properties of ceramides and their impact on the stratum corneum structure: a review. Part 1: ceramides. Skin Pharmacol Physiol 20:220–229

Wegener M, Neubert R, Rettig W, Wartewig S (1997) Structure of stratum corneum lipids characterized by FT-raman spectroscopy and DSC. III. Mixtures of ceramides and cholesterol. Chem Phys Lipids 88:73–82

Wertz PW, Downing DT (1983) Ceramides of pig epidermis: structure determination. J Lipid Res 24:759–765

Wertz PW, Swartzendruber DC, Madison KC, Downing DT (1987) Composition and morphology of epidermal cyst lipids. J Invest Dermatol 89:419–425

White SH, Mirejovsky D, King GI (1988) Structure of lamellar lipid domains and corneocyte envelopes of murine stratum corneum. An x-ray diffraction study. Biochemistry 27:3725–3732

Wiener MC, White SH (1991) Fluid bilayer structure determination by the combined use of x-ray and neutron-diffraction. 1. Fluid bilayer models and the limits of resolution. Biophys J 59:162–173

Worcester DL (1976) Neutron diffraction studies of biological membranes and membrane components. Brookhaven Symp Biol 27:III37–III57

Yamamoto A, Serizawa S, Ito M, Sato Y (1991) Stratum corneum lipid abnormalities in atopic dermatitis. Arch Dermatol Res 283:219–223

Zbytovska J, Vavrova K, Kiselev MA, Lessieur P, Wartewig S, Neubert RHH (2009) The effects of transdermal permeation enhancers on thermotropic phase behaviour of a stratum corneum lipid model. Colloids Surf A 351:30–37

Zemlyanaya EV, Kiselev MA, Neubert R, Kohlbrecher J, Aksenov VL (2008) Investigation of the structure and properties of model membranes of the stratum corneum by small-angle neutron scattering. J Surf Invest X-Ray 2:884–889